

## Excited-State Hydrogen and Dihydrogen Bonding of a Dihydrogen-Bonded Phenol–Borane–Dimethylamine Complex

Yufang Liu,<sup>\*1</sup> Yonggang Yang,<sup>1,2</sup> Kai Jiang,<sup>2</sup> Deheng Shi,<sup>1</sup> and Jinfeng Sun<sup>1</sup>

<sup>1</sup>Department of Physics, Henan Normal University, Xinxiang 453007, P. R. China

<sup>2</sup>Department of Chemistry, Henan Normal University, Xinxiang 453007, P. R. China

Received August 19, 2010; E-mail: yf-liu@henannu.edu.cn

The excited-state hydrogen and dihydrogen bonding of a dihydrogen-bonded phenol–borane–dimethylamine (BDMA) complex was investigated theoretically by use of time-dependent density functional theory (TDDFT). The coexistence of an intermolecular dihydrogen bond (B–H...H–O) and hydrogen bond (N–H...O) was confirmed by the optimized geometric structure of the dihydrogen-bonded phenol–BDMA complex. The infrared spectra for both the ground and excited states of the dihydrogen-bonded phenol–BDMA complex were also calculated by use of density functional theory (DFT)/TDDFT. As a result, we demonstrated theoretically that the intermolecular dihydrogen bonds B–H...H–O can be significantly strengthened in the excited state. However, the intermolecular hydrogen bond N–H...O in the dihydrogen-bonded phenol–BDMA complex is weakened upon photoexcitation to the  $S_1$  state. The dynamic changes of the intermolecular dihydrogen and hydrogen bonding are consistent with the calculated bond lengths in different electronic states. The coexistent dihydrogen and hydrogen bonding in the electronic excited states of this dihydrogen-bonded complex was studied theoretically in this work. Furthermore, it was found that the N–H...O hydrogen bond in the cyclic structure of phenol–BDMA complex hindered the dehydrogenation reaction between dihydrogen bonded O–H and B–H<sub>1</sub> groups, which has been reported for the phenol–borane–trimethylamine complex.

As a ubiquitous phenomenon in chemistry, biology, and other branches of science, hydrogen bonding plays a crucial role in solute–solvent interactions, recognition in biological macromolecules, and so forth.<sup>1–16</sup> In general, hydrogen bonding can be represented as the interaction between an acidic proton as a proton donor (such as O–H, N–H) and the lone pair of an electronegative element, the  $\pi$  electrons of a multiple bond or aromatic ring, or a transition metal center as hydrogen acceptor.<sup>1–16</sup> In contrast to the above, dihydrogen bonding is the interaction between two oppositely charged hydrogen atoms, which can be represented as D–H...H–A, where D and A are, respectively, electronically negative and electronically positive elements with respect to hydrogen.<sup>17–32</sup> For example, D could be a conventional hydrogen donor, such as O and N, and A could be a metal/boron group hydride. Dihydrogen bonding has attracted a great deal of attention in recent years. At the same time, the strength of dihydrogen bonding is analogous to conventional hydrogen bonding. Hence, it has most of the functions of conventional hydrogen bonding as well as some novel features.<sup>17–32</sup> Dihydrogen bonding may be an intermediate in dehydrogenation, which provides some prospects for potential hydrogen storage materials.<sup>33–36</sup> In addition to metal hydrides, dihydrogen bonding is present in a large number of amine–boron derivatives, which have become a hotspot attracting the attention of many researchers.<sup>33,37–47</sup>

Moreover, boron amines have only recently received attention for their particular properties and the advantages they give, even though they have been known for a number of years.<sup>34</sup> The dihydrogen bonds between boron–amine and an acidic hydrogen donor, such as phenol, aniline, or 2-pyridone,

have been reported in the gas phase.<sup>41–45</sup> Laser-induced fluorescence (LIF) excitation, fluorescence-detected infrared (FDIR) and infrared–ultraviolet (IR–UV) hole-burning spectroscopies were adopted to study the complex between borane–dimethylamine (BDMA) and phenol, in order to confirm the formation of dihydrogen bonding and work out its mechanism of hydrogen storage.<sup>46</sup> The LIF excitation spectrum of monomer phenol red-shifted 89 cm<sup>–1</sup> upon addition of BDMA, which is small compared to the 384 cm<sup>–1</sup> red shift of borane–trimethylamine (BTMA).<sup>41,42,46</sup> The FDIR spectrum showed a 174 cm<sup>–1</sup> shift toward a lower frequency, from 3657 to 3483 cm<sup>–1</sup>, of the O–H stretching mode, which is much larger than that for phenol–H<sub>2</sub>O (133 cm<sup>–1</sup>) and suggests the appearance of dihydrogen bonding between phenol and BDMA.<sup>32,33,37</sup> The IR–UV hole-burnt spectra demonstrated that there is only one isomer for phenol–BDMA under the present experimental conditions.<sup>41,46</sup> At the same time, *ab initio* and density functional theory (DFT) calculations were carried out to study the dihydrogen bonding between phenol and BDMA; from this, the presence of three isomers was ascertained, and by comparing their bonding energies and other properties, it was shown that the cyclic system should be the most stable one which has both hydrogen and dihydrogen bonds.<sup>41,46</sup>

Many studies have been performed to study the properties of dihydrogen-bonded complexes using both experimental methods, such as LIF excitation, FDIR spectroscopy, IR–UV hole-burning spectroscopy, nuclear magnetic resonance, and theoretical methods to obtain information on their dynamics and their potential hydrogen storage mechanism.<sup>24–46</sup> However,

there have been few studies on the properties of dihydrogen-bonded complexes in their electronic excited state. Recently, Zhao et al. reported a theoretical study on the structure and dynamics of a novel dihydrogen bond in the electronically excited state of a phenol–BTMA complex.<sup>47</sup> In their benchmark study, time-dependent density functional theory (TDDFT) revealed that the dihydrogen-bonded phenol–BTMA complex possesses a locally excited (LE)  $S_1$  state that is centered on the phenol moiety.<sup>47</sup> In addition, there was no O–H or B–H stretching vibrational mode in the calculated infrared (IR) spectrum of the  $S_1$  state of the dihydrogen-bonded phenol–BTMA complex. This was attributed to the significant hydrogen bond strengthening of the dihydrogen bond O–H...H–B in the electronic excited state.

In this work, we investigated theoretically the dihydrogen-bonded phenol–BDMA complex in both the ground state and electronic excited states by use of DFT and TDDFT methods, which have been proven reliable tools for the analysis of large dihydrogen-bonded complexes in the ground and excited states.

### Computational Methods

The TURBOMOLE program suite was used to calculate electronic structures, vibration and absorption spectra, molecular orbitals, and other information.<sup>11,48–55</sup> Both in DFT for the ground state and TDDFT for excited state, the generalized gradient approximation (GGA) was employed for the exchange correlation potential (B-P86).<sup>48</sup> It has been reported that B-P86 functional was probably best for the whole of chemistry.<sup>49</sup> Furthermore, it has been used by many researchers for the study of hydrogen bonding and dihydrogen bonding in both ground and excited states, and many reliable results have been calculated according to experimental results.<sup>4,7,8,11,50,51</sup> To improve the efficiency, the resolution-of-the-identity (RI) approximation was applied without sacrificing accuracy.<sup>48,52–54</sup> The triple- $\zeta$  valence quality with one set of polarization functions (TZVP) were chosen as the basis sets and the corresponding auxiliary basis sets for the RI approximation throughout.<sup>54</sup> Harmonic vibrational frequencies in the ground and excited state were determined by diagonalization of the Hessian.<sup>55</sup> Through the numerical differentiation of analytical gradients using central differences and default displacements of 0.02 Bohr, the excited state Hessian was obtained. The infrared intensities were determined from the gradients of the dipole moment.<sup>48,55</sup>

### Results and Discussion

#### Geometric Structures in Ground and Excited States.

Borane amine derivatives have recently attracted significant attention for their ability to form dihydrogen bonding and their potential to store  $H_2$  by forming a dihydrogen-bonded complex or intermediate of dihydrogen elimination reactions.<sup>37–47</sup> Hence, the dihydrogen-bonded phenol–BDMA complex was studied theoretically here. The fully optimized geometric structure of the dihydrogen-bonded phenol–BDMA is shown in Figure 1 and the corresponding structural information is presented in Table 1.

In Figure 1, the cyclic structure of dihydrogen-bonded phenol–BDMA, which consists of both hydrogen bond and dihydrogen bonds, can be seen. The B–H bond length of the

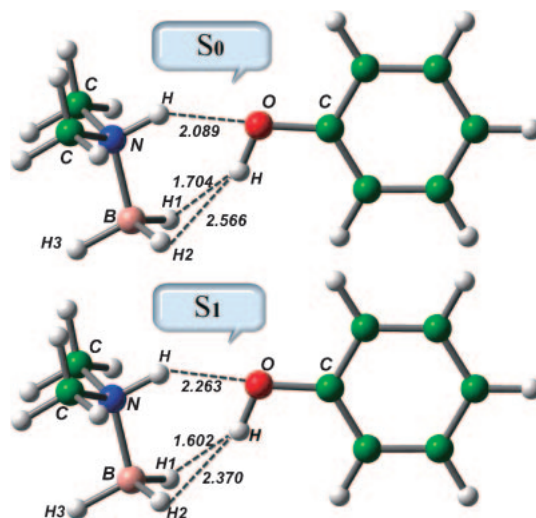


**Figure 1.** The optimized geometric structure of dihydrogen-bonded phenol–BDMA in both ground state and  $S_1$  state with calculated bond lengths (in Å) of  $H_1\cdots H$ ,  $H_2\cdots H$ , and  $N-H\cdots O$ .

monomer BDMA was almost the same at about 1.220 Å for its  $C_3$  symmetry in the ground state. This changed with the formation of the dihydrogen bond, both B– $H_2$  and B– $H_3$  shortened from 1.220 to 1.216 Å, while the B– $H_1$  lengthened from 1.219 to 1.232 Å which formed the strongest dihydrogen bond. Additionally, the O–H group of phenol lengthened by 0.016 Å from 0.974 Å, while the C–O group shortened from 1.376 to 1.374 Å because of the dihydrogen bond. Moreover, the distance between the two hydrogen atoms in the dihydrogen-bonded complex was 1.704 and 2.566 Å for  $H_1\cdots H$  and  $H_2\cdots H$ , respectively, both of which were shortened to 1.602 and 2.370 Å when excited to the  $S_1$  state, showing that both the dihydrogen bonds were strengthened. For the dihydrogen bond of B– $H_1\cdots H$ , the bent angles of  $BH_1H$  and  $OHH_1$  were about 106 and 149°, respectively, and the bond length was 1.704 Å, in accordance with the structure of that reported whereby the H–H contact distance was less than 2.4 Å (the sum of the van der Waals radii) and the strongly bent angles averaged around 110 and 150°. The above analysis confirmed the formation of the dihydrogen bond for phenol–BDMA. Also, we can see that the bond length of N–H lengthened from 1.026 to 1.032 Å and the hydrogen bond N–H...O was 2.089 Å long, which leads to the conclusion that the hydrogen bond also exists in the phenol–BDMA complex. Above all, it confirmed that phenol–BDMA possessed a cycle system with both hydrogen and dihydrogen bonds, which is in agreement with the experimental conclusions. In the  $S_1$  state, the dihydrogen bond between  $H_1\cdots H$  and  $H_2\cdots H$  shortened by 0.102 and 0.196 Å, respectively, but the hydrogen bond N–H...O lengthened compared to the ground state. We may conclude that phenol tends toward the borane and away from the ammonia. This is because of enhancing of the dihydrogen bond and the weakening of the hydrogen bond in the excited state; this can also be proven by the dipole moment changing from 1.4689 in the ground state to 1.6886 in the excited  $S_1$  state, which is observed by comparing it with the phenol–BTMA complex in the excited state which undergoes dehydrogenation.<sup>47,56</sup> There-

**Table 1.** Calculated Bond Lengths  $L$  (in Å) for the Dihydrogen-Bonded Phenol–BDMA in Ground and Excited State, Also Isolated Phenol and BDMA in Ground State Are Shown

	$L_{B-H3}$	$L_{B-H2}$	$L_{B-H1}$	$L_{N-H}$	$L_{N-H\cdots O}$	$L_{H1\cdots H}$	$L_{H2\cdots H}$	$L_{O-H}$	$L_{C-O}$
Monomers	1.220	1.220	1.219	1.026				0.974	1.376
Complex ( $S_0$ )	1.216	1.216	1.232	1.032	2.089	1.704	2.566	0.990	1.374
Complex ( $S_1$ )	1.214	1.216	1.234	1.030	2.263	1.602	2.370	1.004	1.368

**Table 2.** Calculated Electronic Transition Energies (in eV) and Corresponding Oscillation Strengths (in the Parentheses) for the Dihydrogen-Bonded Phenol–BDMA, and Monomers<sup>a)</sup>

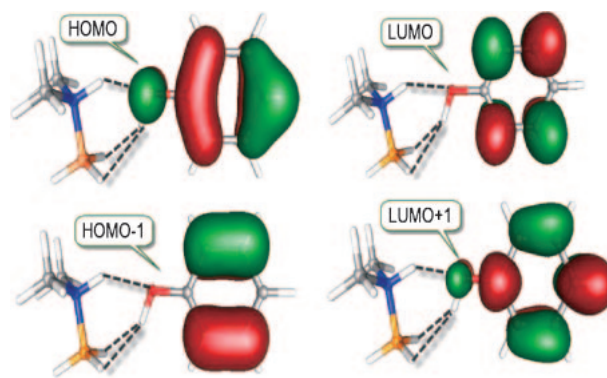
	Phenol	Phenol–BDMA	BDMA
$S_1$	4.788 (0.031)	4.796 (0.026)	6.114 (0.007)
	H $\rightarrow$ L 82.5%	H $\rightarrow$ L 81.9%	H $\rightarrow$ L 99.9%
	H-1 $\rightarrow$ L+1 16.6%	H-1 $\rightarrow$ L+1 17.2%	
$S_2$	5.684 (0.049)	5.407 (0.003)	6.158 (0.011)
$S_3$	5.781 (0.000)	5.619 (0.003)	7.270 (0.018)
$S_4$	6.468 (0.000)	5.645 (0.100)	7.332 (0.007)
$S_5$	6.506 (0.215)	5.726 (0.001)	7.790 (0.006)
$S_6$	6.573 (0.001)	6.009 (0.001)	7.839 (0.005)

a) Also, the orbital transition contributions for the  $S_1$  state are also listed.

fore, we can conclude that the hydrogen bond  $N-H\cdots O$  hindered the phenol toward the borane and caused the elimination of hydrogen even though it weakened in the excited state. This suggests that there is potential for the borane amine to act as a hydrogen storage and hydrogen release intermediate through the information of a dihydrogen bond by the replacement of methyl and hydrogen.

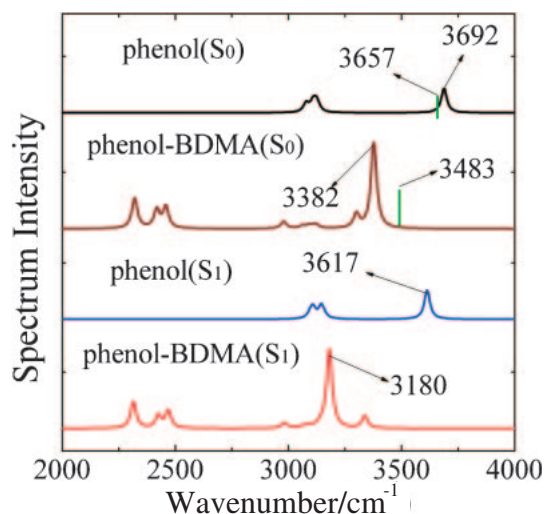
**The Transition Energy and Frontier Molecular Orbital Analysis.** Electronic transition energies and corresponding oscillation strengths calculated by TDDFT for the dihydrogen-bonded phenol–BDMA and monomers are shown in Table 2. It can be seen that the electronic transition for the  $S_1$  state of the dihydrogen-bonded phenol–BDMA (4.796) is very close to the transition energy for the  $S_1$  state of the monomer phenol (4.788), while is much lower than the transition energy for the  $S_1$  state of the monomer BDMA (6.114). Therefore, we may conclude that in dihydrogen-bonded phenol–BDMA only the phenol moiety was electronically excited to the  $S_1$  state, while the BDMA moiety was in its ground state. In addition, the orbital transition contributions of dihydrogen-bonded phenol–BDMA in the  $S_1$  state are also listed in Table 2, where we note that the  $S_1$  state mainly contributes to the highest occupied molecular orbital (HOMO) to lowest unoccupied molecular orbital (LUMO) transition in 81.9%, while the orbital transition from HOMO–1 to LUMO+1 possesses a small proportion, about 17.2%. The analysis for the four molecular orbitals hereinafter may provide more information about the change of the electron cloud in the  $S_1$  state.

Figure 2 presents the frontier molecular orbitals of dihydrogen-bonded phenol–BDMA. From the TDDFT results, the four molecular orbitals can contribute to the electronic transition to the  $S_1$  state. One can note that the electron densities of molecular orbitals were all localized in the phenol moiety, which makes it clear that the  $S_1$  state of dihydrogen-

**Figure 2.** Frontier molecular orbital (MOs) of the dihydrogen-bonded phenol–BDMA complex.

bonded phenol–BDMA is a locally excited (LE) state. At the same time, it can be seen that the lone pair electron of the hydroxy group which engages in the formation of the dihydrogen bond is also electronically excited to the benzene ring moiety. This indicates that the dihydrogen bond may be strongly affected by the electron distribution due to the electronic transition. It can be seen that the electron densities of hydroxy group decreased after the HOMO  $\rightarrow$  LUMO transition. Therefore, the interaction of the dihydrogen bondings  $B-H^{\delta-}_1\cdots^{\delta+}H-O$  and  $B-H^{\delta-}_2\cdots^{\delta+}H-O$  strengthened after the excitation, while the interaction of hydrogen bonding  $N-H^{\delta+}\cdots^{\delta-}O$  weakened. These interactions induced strengthening of dihydrogen bondings and weakening of hydrogen bonding respectively.

**Infrared Spectra of Complex and Monomers in Ground and Excited State.** Figure 3 shows the calculated infrared spectra of the monomer phenol and dihydrogen-bonded complex in the ground and  $S_1$  states. Herein, for the monomer phenol in the ground state, the stretching vibration of O–H was calculated to be  $3692\text{ cm}^{-1}$ , which is in good agreement with the experimental value of  $3657\text{ cm}^{-1}$ .<sup>33,37</sup> The O–H stretching vibration of is red-shifted by  $75\text{ cm}^{-1}$  in the  $S_1$  state. Upon the formation of the dihydrogen bond, the stretching vibration frequency of O–H shifts to the red by  $310\text{ cm}^{-1}$  from  $3692$  to  $3382\text{ cm}^{-1}$  in the ground state. The red shift induced by the formation of the dihydrogen bond becomes larger in the  $S_1$  state ( $512\text{ cm}^{-1}$ ). It can be confirmed that the dihydrogen bonding between O–H and H–B and the dihydrogen bonding is significantly strengthened when it is excited to the  $S_1$  state due to the larger red shift of the O–H stretching mode in comparison with that in the ground state. In addition, it is clear that the stretching vibration mode of O–H does not disappear in the excited state of phenol–BDMA, which is different from the dihydrogen-bonded phenol–BTMA system.<sup>38</sup>



**Figure 3.** Calculated infrared spectra of monomer phenol and dihydrogen-bonded phenol-BDMA complex in different electronic state. The green line denotes the experiment values.

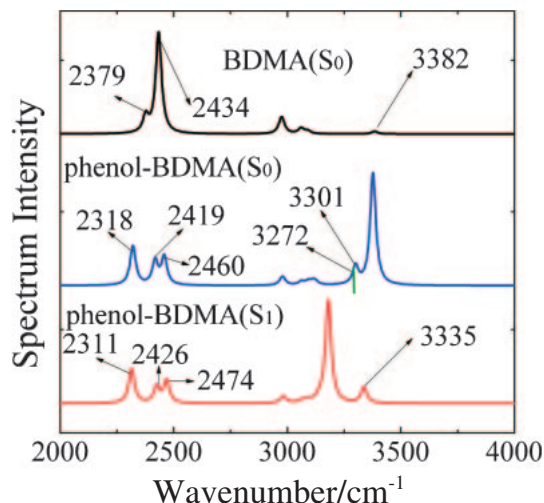


**Figure 4.** Calculated infrared spectra of monomer BDMA and dihydrogen-bonded phenol-BDMA in ground state and  $S_1$  state. The green line denotes the experiment values.

The infrared spectra of the monomer BDMA and dihydrogen-bonded phenol-BDMA complex in the ground state and  $S_1$  state are shown in Figure 4. One can note that in the ground state of the monomer BDMA the absorption peaks of 2379 and 2434  $\text{cm}^{-1}$  should correspond to the B-H group, with B-H<sub>2</sub> and B-H<sub>3</sub> located at higher frequency while the B-H<sub>1</sub> corresponds to 2379  $\text{cm}^{-1}$ , and the 3382  $\text{cm}^{-1}$  absorption peak should be ascribed to the N-H group. It can be seen that the stretching vibration frequency of the N-H group red shifts to 3301  $\text{cm}^{-1}$  from 3382  $\text{cm}^{-1}$  due to the hydrogen bond formation of phenol-BDMA in the ground state. In the  $S_1$  state, this value blue shifts by 34  $\text{cm}^{-1}$  to a higher frequency, which indicates that the hydrogen bond may be weakened upon photoexcitation. This is in agreement with the bond length change in different states. On the other hand, the higher stretching vibration absorption of the B-H group was disrupted into two

absorption peaks due to the formation of the dihydrogen bond, at 2419 and 2460  $\text{cm}^{-1}$ , while the stretching mode B-H<sub>1</sub> red shifts by 61  $\text{cm}^{-1}$ . In the  $S_1$  state, both the stretching mode B-H<sub>2</sub> and B-H<sub>3</sub> blue shift to higher frequencies: 2426 and 2474  $\text{cm}^{-1}$ , respectively. This is also consistent with the change in the bond length. In addition, the stretching mode of the B-H<sub>1</sub> shifts to a lower frequency in the excited state than that in the ground state. Hence, the dihydrogen bond O-H...H<sub>1</sub>-B is strengthened in the excited  $S_1$  state.

### Conclusion

In summary, TDDFT was employed to study excited-state hydrogen and dihydrogen bonding in a dihydrogen-bonded phenol-BDMA complex. From the optimized geometric structure of the dihydrogen-bonded phenol-BDMA complex, both the formation of the intermolecular dihydrogen bond (B-H...H-O) and the hydrogen bond (N-H...O) in the cyclic complex were confirmed. From the TDDFT results, it was demonstrated that the  $S_1$  state is an LE state. The infrared spectra of the dihydrogen-bonded phenol-BDMA complex were also calculated by use of TDDFT. The stretching vibration frequency for O-H in the dihydrogen-bonded phenol-BDMA complex could induce a larger red shift by the formation of intermolecular hydrogen bond B-H...H-O in the  $S_1$  state than that in the ground state. Thus, it was demonstrated that the intermolecular dihydrogen bonds B-H...H-O can be significantly strengthened in the excited state. Nevertheless, the stretching mode N-H blue shifts by 38  $\text{cm}^{-1}$  in the  $S_1$  state compared to that in the ground state. Hence, this demonstrates that the intermolecular hydrogen bond N-H...O is weakened upon photoexcitation to the  $S_1$  state. The dynamic changes of the intermolecular dihydrogen and hydrogen bonding are consistent with the calculated bond lengths in different electronic states. This is the first report of a theoretical study of the excited-state coexistent dihydrogen and hydrogen bonding in a novel dihydrogen-bonded complex and their interaction with each other in a cyclic structure.

This work was supported by the National Natural Science Foundation of China (Grant No. 60977063), the Innovation Scientists and Technicians Troop Construction Projects of Henan Province, China (Grant No. 084100510011).

### References

- 1 I. L. Karle, *J. Mol. Struct.* **1999**, 474, 103.
- 2 B. Luisi, M. Orozco, J. Sponer, F. J. Luque, Z. Shakked, *J. Mol. Biol.* **1998**, 279, 1123.
- 3 A. D. Buckingham, J. E. Del Bene, S. A. C. McDowell, *Chem. Phys. Lett.* **2008**, 463, 1.
- 4 G.-J. Zhao, K.-L. Han, *J. Phys. Chem. A* **2007**, 111, 2469.
- 5 G.-J. Zhao, K.-L. Han, *J. Phys. Chem. A* **2007**, 111, 9218.
- 6 T. K. Ghanty, V. N. Staroverov, P. R. Koren, E. R. Davidson, *J. Am. Chem. Soc.* **2000**, 122, 1210.
- 7 G.-J. Zhao, J.-Y. Liu, L.-C. Zhou, K.-L. Han, *J. Phys. Chem. B* **2007**, 111, 8940.
- 8 G.-J. Zhao, K.-L. Han, *Biophys. J.* **2008**, 94, 38.
- 9 S. Chai, G.-J. Zhao, P. Song, S.-Q. Yang, J.-Y. Liu, K.-L. Han, *Phys. Chem. Chem. Phys.* **2009**, 11, 4385.
- 10 S. Mukherjee, S. Majumdar, D. Bhattacharyya, *J. Phys.*

*Chem. B* **2005**, 109, 10484.

11 Y. Liu, J. Ding, R. Liu, D. Shi, J. Sun, *J. Photochem. Photobiol., A* **2009**, 201, 203.

12 G.-J. Zhao, K.-L. Han, P. J. Stang, *J. Chem. Theory Comput.* **2009**, 5, 1955.

13 L.-C. Zhou, G.-J. Zhao, J.-F. Liu, K.-L. Han, Y.-K. Wu, X.-J. Peng, M.-T. Sun, *J. Photochem. Photobiol., A* **2007**, 187, 305.

14 Y.-H. Liu, G.-J. Zhao, G.-Y. Li, K.-L. Han, *J. Photochem. Photobiol., A* **2010**, 209, 181.

15 G.-J. Zhao, K.-L. Han, *J. Comput. Chem.* **2008**, 29, 2010.

16 G.-J. Zhao, K.-L. Han, *J. Phys. Chem. A* **2009**, 113, 14329.

17 E. V. Bakhmutova, V. I. Bakhmutov, N. V. Belkova, M. Besora, L. M. Epstein, A. Lledós, G. I. Nikonov, E. S. Shubina, J. Tomàs, E. V. Vorontsov, *Chem.—Eur. J.* **2004**, 10, 661.

18 F. Fuster, B. Silvi, S. Berski, Z. Latajka, *J. Mol. Struct.* **2000**, 555, 75.

19 A. H. Pakiari, Z. Jamshidi, *THEOCHEM* **2004**, 685, 155.

20 H. Jacobsen, *Chem. Phys.* **2008**, 345, 95.

21 M. G. Govender, T. A. Ford, *THEOCHEM* **2003**, 630, 11.

22 N. V. Belkova, T. N. Gribanova, E. I. Gutsul, R. M. Minyaev, C. Bianchini, M. Peruzzini, F. Zanobini, E. S. Shubina, L. M. Epstein, *J. Mol. Struct.* **2007**, 844–845, 115.

23 Y. Wu, L. Feng, X. Zhang, *THEOCHEM* **2008**, 851, 294.

24 S. Gao, W. Wu, Y. Mo, *J. Phys. Chem. A* **2009**, 113, 8108.

25 S. J. Grabowski, W. A. Sokalski, J. Leszczynski, *J. Phys. Chem. A* **2005**, 109, 4331.

26 S. A. Kulkarni, *J. Phys. Chem. A* **1998**, 102, 7704.

27 P. C. Singh, D. K. Maity, G. N. Patwari, *J. Phys. Chem. A* **2008**, 112, 5930.

28 S. A. Kulkarni, A. K. Srivastava, *J. Phys. Chem. A* **1999**, 103, 2836.

29 S. J. Grabowski, W. A. Sokalski, J. Leszczynski, *J. Phys. Chem. A* **2004**, 108, 5823.

30 P. L. A. Popelier, *J. Phys. Chem. A* **1998**, 102, 1873.

31 T. B. Richardson, S. de Gala, R. H. Crabtree, P. E. M. Siegbahn, *J. Am. Chem. Soc.* **1995**, 117, 12875.

32 R. Custelcean, J. E. Jackson, *J. Am. Chem. Soc.* **1998**, 120, 12935.

33 D. A. Dixon, M. Gutowski, *J. Phys. Chem. A* **2005**, 109, 5129.

34 M. T. Nguyen, V. S. Nguyen, M. H. Matus, G. Gopakumar,

D. A. Dixon, *J. Phys. Chem. A* **2007**, 111, 679.

35 X.-B. Zhang, S.-Q. Shi, L. Jiang, S. Han, Y. Kotani, T. Kiyobayashi, N. Kuriyama, T. Kobayashi, Q. Xu, *J. Phys. Chem. C* **2007**, 111, 5064.

36 S. Gründemann, S. Ulrich, H.-H. Limbach, N. S. Golubev, G. S. Denisov, L. M. Epstein, S. Sabo-Etienne, B. Chaudret, *Inorg. Chem.* **1999**, 38, 2550.

37 S. Trudel, D. F. R. Gilson, *Inorg. Chem.* **2003**, 42, 2814.

38 W. T. Klooster, T. F. Koetzle, P. E. M. Siegbahn, T. B. Richardson, R. H. Crabtree, *J. Am. Chem. Soc.* **1999**, 121, 6337.

39 Y. Meng, Z. Zhou, C. Duan, B. Wang, Q. Zhong, *THEOCHEM* **2005**, 713, 135.

40 P. C. Singh, G. N. Patwari, *Chem. Phys. Lett.* **2006**, 419, 5.

41 G. N. Patwari, T. Ebata, N. Mikami, *Chem. Phys.* **2002**, 283, 193.

42 G. N. Patwari, T. Ebata, N. Mikami, *J. Chem. Phys.* **2000**, 113, 9885.

43 P. C. Singh, G. N. Patwari, *J. Phys. Chem. A* **2007**, 111, 3178.

44 G. N. Patwari, *J. Phys. Chem. A* **2005**, 109, 2035.

45 G. N. Patwari, T. Ebata, N. Mikami, *J. Phys. Chem. A* **2001**, 105, 8642.

46 G. N. Patwari, T. Ebata, N. Mikami, *J. Chem. Phys.* **2002**, 116, 6056.

47 G.-J. Zhao, K.-L. Han, *J. Chem. Phys.* **2007**, 127, 024306.

48 F. Furche, R. Ahlrichs, *J. Chem. Phys.* **2002**, 117, 7433.

49 R. Ahlrichs, F. Furche, S. Grimme, *Chem. Phys. Lett.* **2000**, 325, 317.

50 N.-N. Wei, C. Hao, Z. Xiu, J. Qiu, *Phys. Chem. Chem. Phys.* **2010**, 12, 9445.

51 N. Wei, P. Li, C. Hao, R. Wang, Z. Xiu, J. Chen, P. Song, *J. Photochem. Photobiol., A* **2010**, 210, 77.

52 J. L. Whitten, *J. Chem. Phys.* **1973**, 58, 4496.

53 B. I. Dunlap, J. W. D. Conolly, J. R. Sabin, *J. Chem. Phys.* **1979**, 71, 3396.

54 O. Vahtras, J. Almlöf, M. W. Feyereisen, *Chem. Phys. Lett.* **1993**, 213, 514.

55 A. Schäfer, C. Huber, R. Ahlrichs, *J. Chem. Phys.* **1994**, 100, 5829.

56 G. N. Patwari, T. Ebata, N. Mikami, *J. Phys. Chem. A* **2001**, 105, 10753.